

Berkeley Seismological Laboratory
Annual Report
July 2008 - June 2009

Contents

1	Director's Report	1
1	Introduction	1
2	History and Facilities	1
3	BSL staff news	3
4	Acknowledgements	3
2	Research Studies	5
1	Tremor-tide Correlations and Near Lithostatic Pore Pressures on the Deep San Andreas Fault	6
2	Detection of Missing Repeating Earthquakes Using Recurrence Elements Analysis	8
3	TerraSAR InSAR Investigation of Active Crustal Deformation	10
4	Creep Measurements on the Concord Fault from PS-InSAR	12
5	Seismicity Changes and Aseismic Slip on the Sunda Megathrust Preceding the M_w 8.4 2007 Earthquake	14
6	Moment Moment Tensors for Very Long Period Signals at Etna Volcano, Italy	16
7	Temporal Variations in Crustal Scattering Structure near Parkfield, California, from Receiver Functions	18
8	Remote Triggering of Fault-Strength Changes on the San Andreas Fault at Parkfield	20
9	Source Analysis of the Memorial Day Explosion, Kimchaek, North Korea	22
10	Towards a continuous seismic wavefield scanning	24
11	The rupture process of the Parkfield SAFOD target earthquakes obtained from the empirical Greens function waveform inversion method	26
12	Nonvolcanic Tremor Evolution in the Parkfield, CA Region	28
13	Stability of Local and Regional Coda: Application to the Wells, Nevada Sequence	30
14	Anomalous Moment Tensor Solutions for The Geysers, CA	32
15	Statistical Testing of Theoretical Rupture Models Against Kinematic Inversions	34
16	Testing ElarmS in Japan	36
17	Real-time Earthquake Detection and Hazard Assessment by ElarmS Across California	38
18	Joint Inversion of Group Velocity Dispersion and Long Period Waveforms for Upper Mantle Structure	40
19	Reactivation of an Archean Craton: Constraints from P- and S-wave Tomography in North China . .	42
20	Plume vs. Plate: Convection Beneath the Pacific Northwest	44
21	Imaging Shallow Cascadia Structure with Ambient Noise Tomography	46
22	Seismic Anisotropy Beneath Cascadia and the Mendocino Triple Junction: Interaction of the Subducting Slab with Mantle Flow	48
23	Recovering the Attenuation of Surface Waves from One-Bit Noise Correlations: A Theoretical Approach	50
24	The Origin of Seismic Anisotropy in the D"	52
25	Toward a 3D Global Attenuation Model in the Lower Mantle from the Earth's Free Oscillations	54
26	Anisotropic North American Lithosphere and its Boundary with Asthenosphere	56
27	Crustal Stress and Mechanical Anisotropy of the Lithosphere in Western North America	58
28	Berkeley 3-D Isotropic and Anisotropic S-velocity Model of North American Upper Mantle, Updated to June 2008	61
29	Weak Mantle in NW India Probed by Postseismic GPS Measurements Following the 2001 Bhuj Earthquake	63
30	Comprehensive Test Ban Monitoring: Contributions from Regional Moment Tensors to Determine Source Type and Depth	66

6 Moment Moment Tensors for Very Long Period Signals at Etna Volcano, Italy

Margaret Hellweg, Andrea Cannata (INGV, Catania), Stefano Gresta (Universita Catania), Sean Ford, Guiseppe Di Grazia (INGV, Catania)

6.1 Introduction

Very long period signals (VLP, 10 s - 30 s) associated with long period events (0.5 Hz - 5 Hz) were observed at Etna Volcano, Italy, during June-November 2005. They are only recorded at the broadband stations nearest to Etna's craters, ECPN, EBEL, EPDN and EPLC. These stations are part of the permanent seismic network run by the Catania Section of the Istituto Nazionale di Geofisica e Vulcanologia (INGV). Although the signal-to-noise (S/N) ratio for these VLPs is in general only poor to fair, they seem to recur, and can be classified into two families. We improved the S/N by stacking (see 2008 Annual Report), and determined moment tensors for the VLP events using the complete waveform, full moment tensor inversion program (*Minson and Dreger, 2008*).

6.2 Moment Tensor Results

We calculated both deviatoric and full moment tensors for the VLP stacks of Family I and Family II using the complete waveform inversion code described by *Minson and Dreger (2008)* and synthetic Green's functions for very shallow source depths. The velocity model used to calculate the Green's functions described a simple half-space with a P-wave velocity of 2.0 km/s and a S-wave velocity of 1.2 km/s. A suite of moment tensor inversions was performed at grid points (horizontal spacing 0.25 km; depths in km: 0.25, 0.50, 0.75, 1.0, 1.5) within the volcanic edifice (locations shown in Figure 2.14). The origin of the rectangular grid was the centroid of the four summit stations. Etna's topography was not included in the calculation of the Green's functions.

For both families, the moment tensor solutions with the best variance reduction (VR) were in the same region of the edifice as the locations determined for the VLP events using radial semblance (*Cannata, et al., 2009*). For Family I, the best solutions had VR > 70% and were best explained by sources that are 60-70% isotropic (ISO) (Figure 2.14). For Family II, they had VR > 60% and 60-70% ISO. Deviatoric solutions for both families had much poorer VR and waveform fits were clearly less satisfactory.

In moment tensor inversions, the signal to noise ratio (SNR) of the data is clearly important. Fifteen years of experience of moment tensor analysis in California include small events down to M 3.5 and below (*Hellweg et al., 2006*). Although events along the central San Andreas Fault are known to be purely double couple (DC),

deviatoric moment tensor solutions for small events with low SNR in the band of analysis (10 s - 50 s) may have up to 30% of their energy modeled by a compensated linear vector dipole (CLVD) mechanism. For the VLP

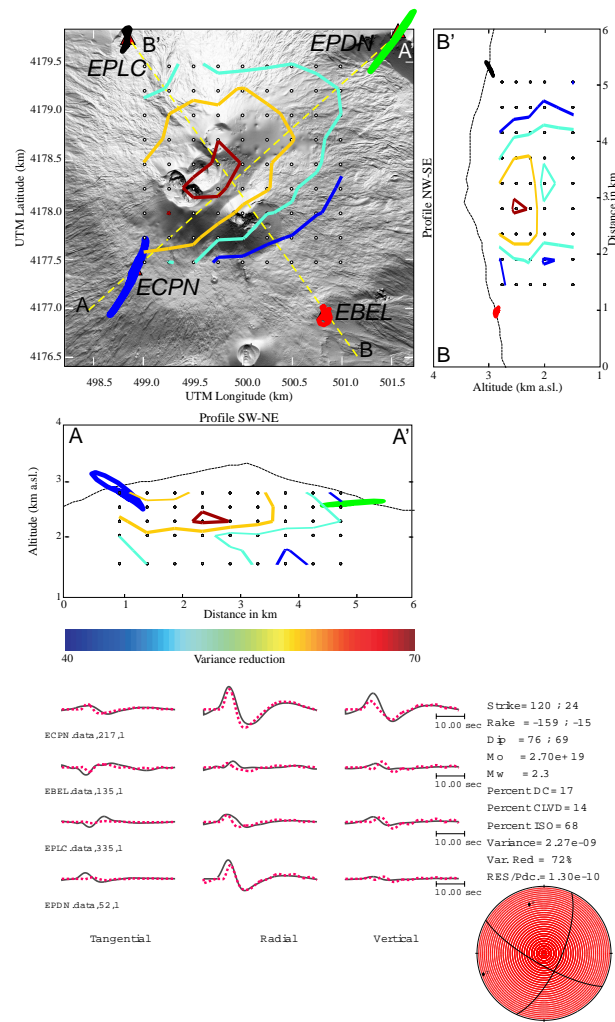


Figure 2.14: Full moment tensor results for Family I events. The map and cross sections show the particle motion at the four summit stations, as well as the search grid and the spatial variation of VR. The source type is plotted on the diamond shaped graph. The bottom panel shows the waveform fits and the mechanism. Note that the amplitudes of the waveforms are scaled so that they can be compared. Results for Family II are very similar.

events of Mt. Etna, even the stacks analysed here, the SNR is low. The DC and CLVD elements of the best solutions vary from grid point to grid point. The eigenvalues describing the deviatoric portions of the solutions also primarily vary randomly in space, with a preference of the largest eigenvector toward a subhorizontal orientation and a slight predominance of SW orientations. Thus, we are convinced that the deviatoric parts of the moment tensor solution are most likely to be efforts of the inversion to explain the noise. They cannot be used to interpret the geometry of the source without better data. There is no reason to suppose that a fit including single-force elements (e.g. *Chouet et al., 2003, Chouet et al., 2005*) would provide greater insight into the source of the VLP events. On “source-type” plots (*Hudson et al., 1989*), it is notable that all of the moment tensor solutions plot somewhere between “explosion” and “opening crack” sources. The scatter gives some sense of the uncertainty in the solutions.

6.3 Perspectives

Using Green’s functions for full moment tensors calculated using a simple half space velocity model, inversions using the algorithm described in *Minson and Dreger (2008)* indicate that a volume change explains a large portion of the waveforms. We intend to follow up with further analysis to investigate the effects of the simple velocity structure, using Green’s functions calculated for the locally used velocity model. We also hope to investigate single source type solutions (i.e. only DC, only CLVD, only ISO), and hope to have longer wavensnippets to improve our understanding of the signal to noise ratio.

6.4 References

Cannata, A., M. Hellweg, G. Di Grazia, S. Ford, S. Alparone, S. Gresta and P. Montalto, Long Period and Very Long Period events at Mt. Etna volcano: characteristics, variability and causality, and implications for their sources, *J. Volcanol. Geotherm. Res.*, in press, 2009.

Chouet, B., P. Dawson, T. Ohminato, M. Martini, G. Saccorotti, F. Giudicepietro, G. De Luca, G. Milana and R. Scarpa, Source mechanism of explosions at Stromboli Volcano, Italy, determined from moment-tensor inversions of very-long-period data, *J. Geophys. Res.* 108, doi:10.1029/20042JB001919, 2003.

Chouet, B., P. Dawson and A. Arciniega-Ceballos, Source mechanism of Vulcanian dagassing at Popocatepetl Volcano, Mexico, determined from waveform inversions of very long period signals, *J. Geophys. Res.* 110, doi:10.1029/2004JB003524, 2005.

Green, D., and J. Neuberg, Waveform classification of volcanic low-frequency earthquake swarms and its implication at Soufriere Hills Volcano, Monserrat, *J. Volcanol. Geotherm. Res.*, 153, 51-63, 2006.

Hellweg, M., D. Dolenc, L. Gee, D. Templeton, M. Xue, D. Dreger and B. Romanowicz, Twelve Years and Counting: Regional Moment Tensors in and around Northern California *Seismol. Res. Lett.*, 77(2), 221, 2006.

Hudson, J.A., R.G. Pearce and R.M. Rogers, Source type plot for inversion of the moment tensor, *J. Geophys. Res.*, 9(B1), 765-774, 1989.

Minson, S. and D. Dreger, Stable Inversions for Complete Moment Tensors, in press *Geophys. Journ. Int.*, 2008.